

Supporting Information

Manganese Dioxide Nanozyme for Reactive Oxygen Therapy of Bacterial Infection and Wound Healing

Li Liu,^{1, #} Cheng Wang,^{1, #} Yuting Li,¹ Lin Qiu,¹ Shuwen Zhou,¹ Pengfei Cui,¹ Pengju Jiang,¹ Xinye Ni,^{2, *} Runhui Liu,³ Xuancheng Du,⁴ Jianhao Wang,^{1, *,} Jiang Xia^{5, *}

¹ School of Pharmacy, Changzhou University, Changzhou, Jiangsu 213164, China.

² The Affiliated Changzhou No. 2 People's Hospital of Nanjing Medical University, Changzhou, Jiangsu, P. R. China

³ State Key Laboratory of Bioreactor Engineering, School of Materials Science and Engineering, East China University of Science and Technology, Shanghai 200237, China.

⁴ Institute of Advanced Interdisciplinary Science, School of Physics, Shandong University, Jinan 250100, China.

⁵ Department of Chemistry, the Chinese University of Hong Kong, Shatin, Hong Kong SAR, China.

[#] These authors contributed equally to this work.

^{*} To whom correspondence may be addressed. Xinye Ni, nxy@njmu.edu.cn; Jianhao Wang, minuswan@163.com; Jiang Xia, jiangxia@cuhk.edu.hk.

Contents

Items	Pages
Figure S1. Color change during the synthesis of OA-MnO ₂ nanozyme.	3
Figure S2. Spectroscopic analysis of the OA-MnO ₂ nanozyme.	4
Figure S3. Stability and catalytic activity of OA-MnO ₂ at different pH.	5
Figure S4. The catalytic stability of OA-MnO ₂ at different temperatures.	6
Figure S5. The catalytic activity of OA-MnO ₂ at different NaCl concentrations.	7
Figure S6. Fluorescence spectra of a TA-containing solution in the absence and presence of OA-MnO ₂ nanozyme.	8
Figure S7. SEM images of <i>S. aureus</i> cells treated by the nanozyme.	9
Figure S8. Biocompatibility of the nanozyme	10

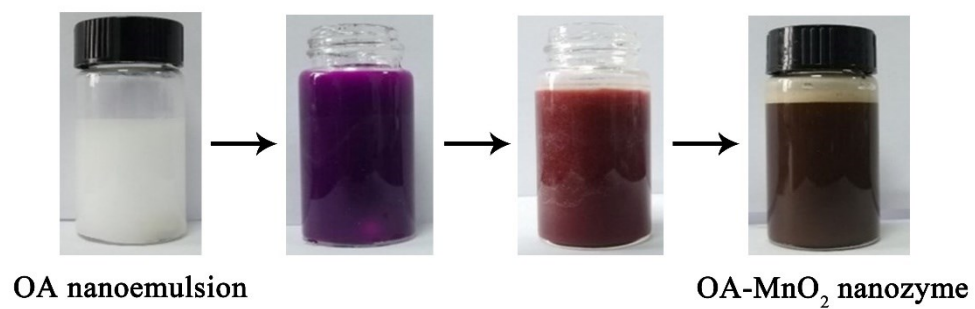


Figure S1. Color change during the synthesis of OA-MnO₂ nanozyme.

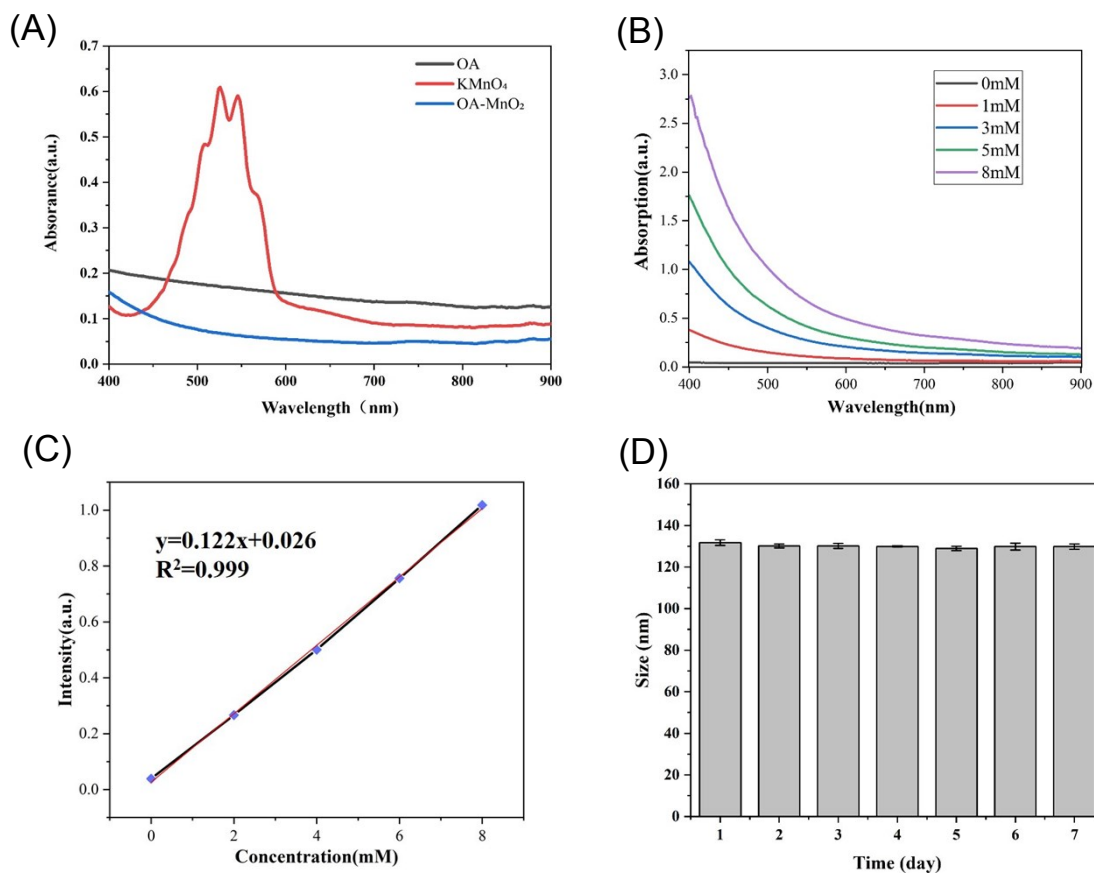


Figure S2. Spectroscopic analysis of the OA-MnO₂ nanozyme. (A) UV-vis absorption spectrum of OA nanoemulsion, pure KMnO₄ and OA-MnO₂ nanozyme. (B) UV-vis absorption spectra of the OA-MnO₂ nanozyme aqueous dispersions with different concentrations. (C) The linear fitting of the absorbance at 500 nm versus concentrations. (D) The hydrodynamic size stability of OA-MnO₂ nanozyme.

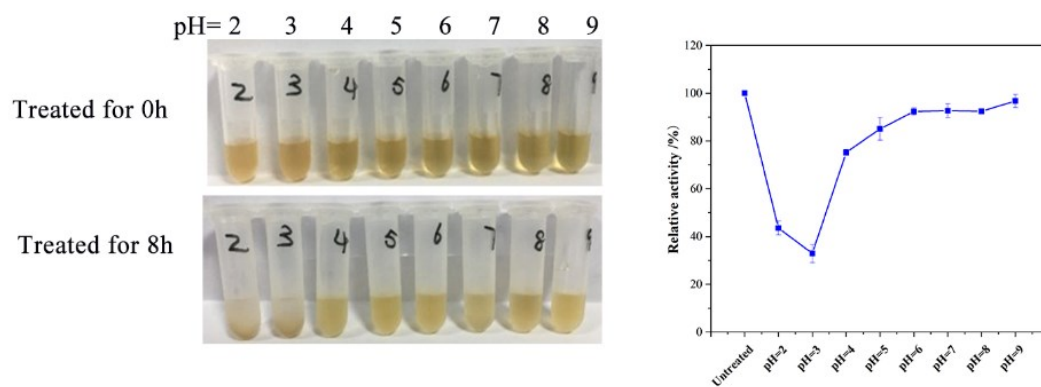


Figure S3. Stability and catalytic activity of OA-MnO₂ at different pH.

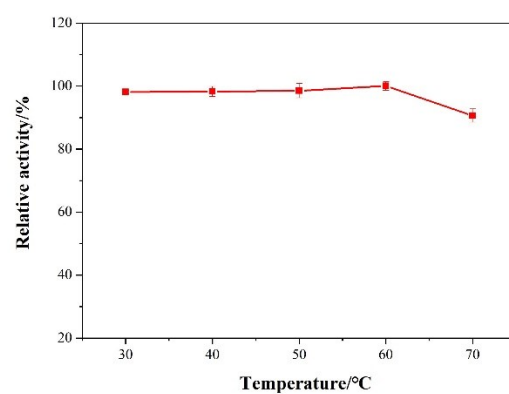


Figure S4. The catalytic stability of OA-MnO₂ at different temperatures.

The concentration of NaCl (M):

0 0.1 0.3 0.4 0.6 0.8 1.0

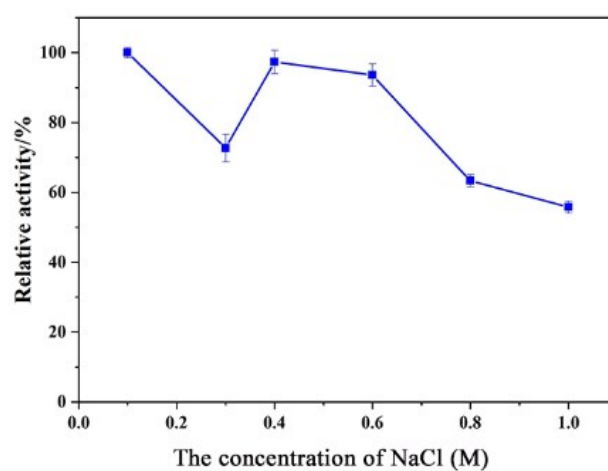
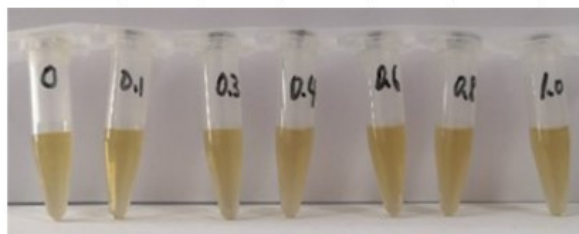


Figure S5. The catalytic activity of OA-MnO₂ at different NaCl concentrations.

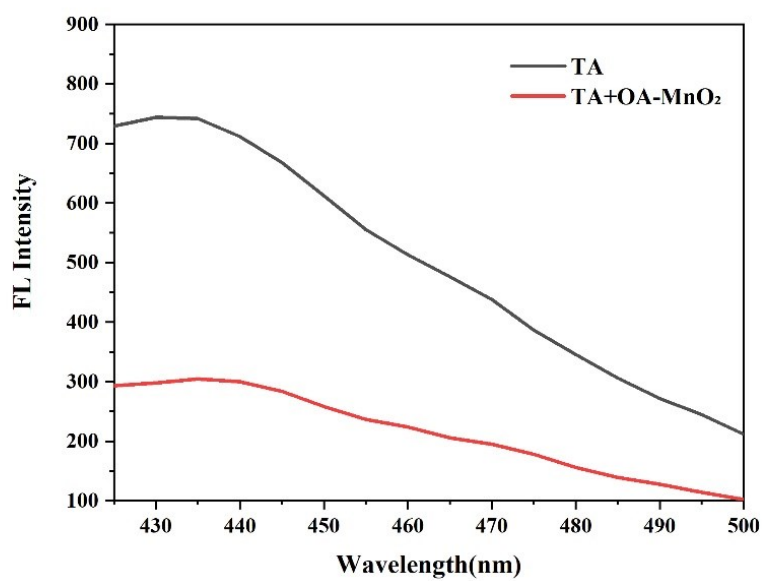


Figure S6. Fluorescence spectra of a TA-containing solution in the absence and presence of OA-MnO₂ nanozyme.

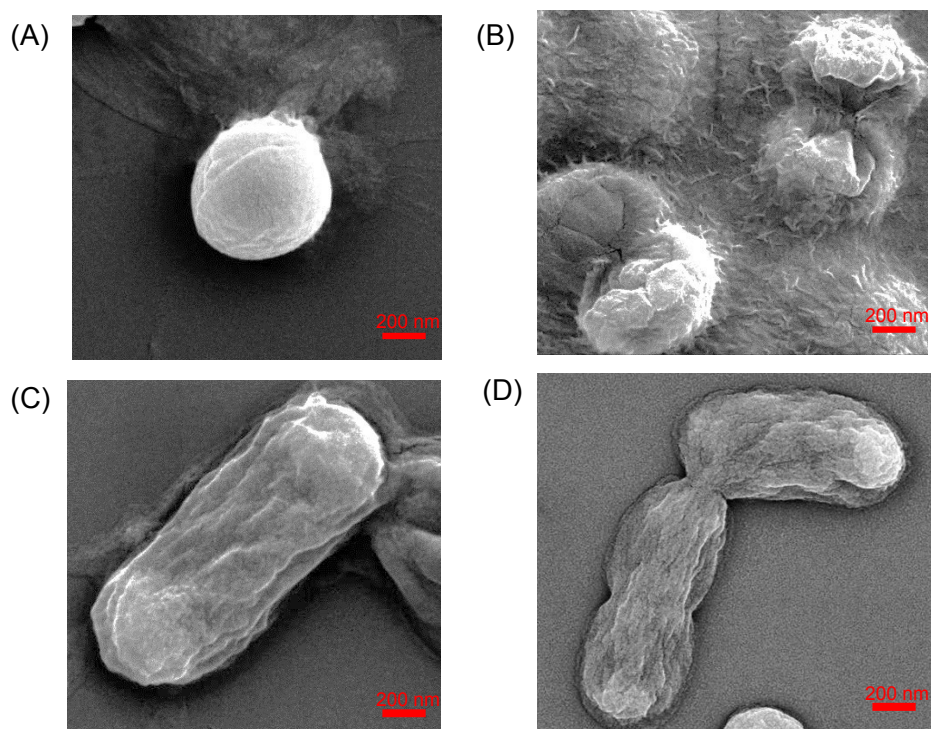


Figure S7. SEM images of *S. aureus* cells treated by the nanozyme. Cells were treated with PBS (A) and OA-MnO₂ nanozyme (8 mM) for 1 h (B), and images of *E. coli* treated with PBS (C) and OA-MnO₂ nanozyme (8 mM) for 1 h (D). Scale bar, 200 nm.

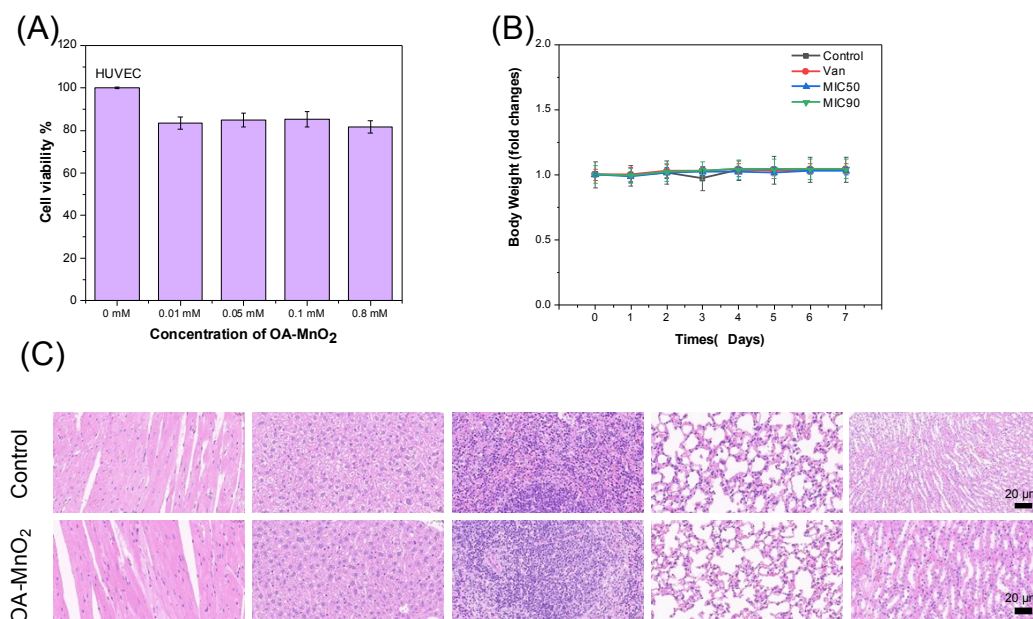


Figure S8. Biocompatibility of the nanozyme. (A) The cytotoxicity of nanozyme towards HUVEC cells measured by the MTT assay. (B) Mice in different treatment groups maintained the body weights during the treatment, indicating a good tolerance to the nanozyme. (C) H&E staining images of major organs (heart, liver, spleen, lung, and kidney) collected from both mice in the control and the MIC₉₀ groups after 7 days showed no detectable difference indicating a low toxicity.